Containment Limits for Free-Inertial Coast

James L. Farrell, *VIGIL Inc.*
Frank van Graas, *Ohio University*

BIOGRAPHIES

James L. Farrell (Ph.D., U. of MD `67; former ION Air Nav representative, senior member of IEEE, former AIAA local board member, member of τβπ, ηκν, πμε) is a registered professional engineering consultant in Maryland. A description of his work experience can be found in http://jameslfarrell.com/james-l-farrell-bio He is author of *GNSS Aided Navigation and Tracking* (2007) (http://jameslfarrell.com) and of *Integrated Aircraft Navigation* (Academic Press, 1976; now in paperback after five printings; http://jameslfarrell.com) plus many columns and papers – http://jameslfarrell.com/wp-content/uploads/2010/06/publist.pdf

Frank van Graas is a Fritz J. and Dolores H. Russ Professor of Electrical Engineering and Principal Investigator with the Avionics Engineering Center at Ohio University. He is an Ohio University Presidential Research Scholar and a Past President of The Institute of Navigation (ION). He received the ION Johannes Kepler and Thurlow awards, and is a Fellow of the ION. He served as the ION Executive Branch Science and Technology Policy Fellow in the Space Communication and Navigation Office at NASA Headquarters during the 2008-2009 academic year. At Ohio, his research interests include all facets of GPS, inertial navigation, LADAR/EO/IR, surveillance and flight test.

ABSTRACT

The paramount importance of safety understandably exerts predominating influence over the establishment of requirements for accuracy and integrity. A central concept involved in setting those requirements is a containment limit; a low probability is assigned for the prospect of flying outside a specified volume during a given phase of flight. Taken literally, that imposes a demand to substantiate maximum allowable values for Total System Error (TSE), a major component of which is navigation error. Risk analyses intended to show satisfaction of those demands are often based on models using gaussian distributions for error contributors, with overbounding to compensate for any possible nonconformance. For free-inertial coast applications, a rigorous mathematical method based on Extreme Value Distributions can achieve overbounding for data sets that are smaller by orders of magnitude than those required for "visual" or binomial bounding techniques.

Extreme Value Theory (EVT) is summarized followed by the application of EVT to derive containment limits for free-inertial coast. Not all inertial error sources, such as vibration-sensitive and misalignment errors, are known or specified, thus justifying the application of EVT to establish containment limits with confidence.

BACKGROUND

Data sets are often obtained from distributions with unknown statistics. In some cases only the parameters are unknown, and the data can be fitted to a common (*e.g.*, gaussian) function. More challenging is the case wherein the specific distribution is likewise unknown. Widespread practices in those instances include fitting the data to an assumed distribution. Immediately that raises an issue regarding outliers. When present in the histogram of available data samples, their values are sometimes

· attributed to purely speculative anomalous conditions – effectively disregarded,
· included in the computation of parameters of the assumed distribution (*e.g.*, mean and σ of a gaussian fit),
· attributed to recognizable anomalous conditions, to justify dismissing them from further consideration.

The first option can obviously risk catastrophic results. The second exercises some caution but invites an ill-fitting distribution to leave unanswered questions about likelihood of worst cases. The third option ignores risk of additional anomalies, possibly present but not yet encountered.

A more subtle risk can arise from two other sources. First, the relevant statistics might not be stationary – parameters of the applicable distribution might not be uniform for all data samples available (or may change before generation of more samples not yet seen). Secondarily the statistics may be stationary but, beyond that, there might be no justification for assuming a distribution within some narrow class. That is especially

true of a gaussian fit assigning extremely low probabilities to sample values far beyond the available data span. With a gaussian fit to non-gaussian data, effects having underestimated severity – unseen as yet – can't be discounted.

Initially it might seem unrealistic to expect successful extraction, from limited available data, of a more general distribution form and also its parameters. Fortunately the means to accomplish that task have been under rigorous development for years. The first few pages of [1] derive the general probability distribution function and subdivide it into three categories associated with names Weibull, Gumbel, and Fréchet. This work applies Fréchet types to free-inertial coast operation.

Prospects of using free-inertial coast as in-flight backup for GPS have been raised in numerous forums and publications. Some studies have stated a case for permitting extended coast durations following loss of GPS coverage. Other efforts have taken a decidedly cautionary direction, due to

· lack of firm commitments in Inertial Measurement Unit (IMU) specifications for various coefficients relevant to error generation, and
· an overriding priority attached to safety.

Publications in the cautionary category have, on occasion, called into question other sources furnishing error budgets intended to justify long coast durations. While no attempt is made here to single out specific sources for criticism, the need for realistic assessment of capability is unequivocally reasserted. This work extends the scope of free-inertial coast investigation, to

· establish a basis for conservative statistical characterization,
· combine that statistical characterization with available analytical modeling tools,
· prepare for validation through flight test.

Previously, EVT was applied to the integrity of Space-Based Augmentation Systems (SBAS) in [2] and [3]. The approach in this paper applies similar tools to free-inertial coast with the justification that inertial error distributions have tails that decay like a power function, which is a necessary condition for the use of EVT.

STATISTICAL ANALYSIS TOOLS

Extremely useful references, including a well-known book [1] plus Internet sources, are used (and paraphrased) herein. Using those sources has been challenging due to considerable differences in notation and various nuances. With absolutely no claim of originality, this document extracts from those references only the information needed to express desired results needed for application to navigation. Since notation is inconsistent (and in a few cases, even ambiguous) among cited references, full

freedom has been assumed here to adopt whatever notation offers the easiest means of explanation.

The methodology involves computation (given a "tail index" – to be described shortly) of quantiles with exceedence probabilities (*i.e.*, instances of samples exceeding prescribed thresholds). The tail index just invoked is defined as the reciprocal of a parameter called the

· extreme value index γ in [1], Eq. (1.1.9) or
· shape parameter ξ in [4], Eq. (1.1).

These cited equations characterize the ***Generalized Extreme Value*** (GEV) distribution. In addition to different nomenclature and notation, they differ in form presented (normalized in [1], not in [4]). The unified representation of the GEV distribution function can be subdivided into the three groups previously noted. Immediately this investigation will focus on the Fréchet distribution, due to its capability for extending a statistical analysis beyond the range of available samples. Extremes not yet been observed but possible [4] are thereby taken into consideration. In this case the shape parameter is greater than zero, and the unified form of the distribution function simplifies to

$$H(x) = e^{-\left(1+\frac{\xi x}{\sigma}\right)^{-\frac{1}{\xi}}}, \xi > 0; 1 + \frac{\xi x}{\sigma} > 0 \qquad (1)$$

Samples of the distribution are to be tested against a threshold u. For values of u approaching the tails of the distribution, the expression just given simplifies further; producing a result having the form of a ***Generalized Pareto Distribution*** (GPD), obtainable by replacing the exponential in (1) with a truncated series representation,

$$G(x) = 1 - B(x),$$

$$B(x) = \left(1 + \frac{\xi x}{\sigma}\right)^{-\frac{1}{\xi}}, x > u \qquad (2)$$

Given the situation $(x > u)$ just cited, the conditional probability that x exceeds the threshold u by an amount up to y is

$$F_u(y) = \frac{Pr(x - u \le y | x > u)}{Pr(x > u)}$$
$$= \frac{F(y+u) - F(u)}{1 - F(u)}, x > u \qquad (3)$$

With above-threshold samples $x = y + u$ and $F_u(y)$ converging to the GPD for large u, that conditional probability is

$$G(x - u) = \frac{F(x) - F(u)}{1 - F(u)} \qquad (4)$$

In these statistical evaluations it is accepted practice to represent the unknown $F(u)$ as $1 - \frac{n}{N}$ where n is the

number of instances ("exceedences over threshold") for which $x > u$ from a sample size N. Thus, in combination with (2), the distribution function $F(x)$ for above-threshold samples and the corresponding above-threshold probability $1 - F(x)$ become simply

$$F(x) = F(u) + [1 - F(u)]G(x - u)$$
$$= 1 - \frac{n}{N} + \frac{n}{N}[1 - B(x - u)] \qquad (5)$$
$$= 1 - \frac{n}{N}B(x - u)$$

$$1 - F(x) = \frac{n}{N}\left[1 + \frac{\xi(x - u)}{\sigma}\right]^{-\frac{1}{\xi}}, x > u \qquad (6)$$

Before completing the derivation, attention is turned to interpretation. The last equation is recognized as the probability of a compound event, resulting from two happenings:

· the threshold is exceeded (probability $\frac{n}{N}$)
· the amount by which the threshold is exceeded is *greater* than x - u . From (2) and (4), $G(x - u)$ is the conditional probability of that amount being less than or equal to $x - u$. The second term is therefore $[1 - G(x - u)]$.

Inverting (6) produces a ***Value at Risk*** (VaR), defined thus:

· from [5]: With statistics of returns denoted r in the context of financial applications, VaR is the worst loss over a specified duration at a chosen confidence level; the value such that, at $(1 - \alpha)$ percentile,

$$Pr(r \leq VaR) = \alpha$$

· from [6]: Largest value of x such that, for some failure probability α at a specified time t

$$Pr\{(loss\ over\ a\ specified\ time\ span) \geq x\} \leq \propto$$

Instead of financial data (r or x above) our application will analyze ensembles of error in a coordinate computed by an inertial navigation system in free-inertial coast. VaR here will therefore be the largest value of that error. Errors accumulated through specified time spans (*e.g.*, beginning with GPS data cutoff and recorded at multiples of five minutes thereafter) will belong to distributions expressed as in (5, 6). Separately for each time span, the probability of error after that duration growing as large as x_α is determined by inversion of (6) with $F(x)$ set to $(1 - \alpha)$:

$$\alpha = \frac{n}{N}\left[1 + \frac{\xi(x_\alpha - u)}{\sigma}\right]^{-\frac{1}{\xi}};$$
$$\frac{N}{n}\alpha = \left[1 + \frac{\xi(x_\alpha - u)}{\sigma}\right]^{-\frac{1}{\xi}}, x_\alpha > u \qquad (7)$$

which is inverted to yield

$$\left(\frac{N}{n}\alpha\right)^{-\xi} - 1 = \left(\frac{n}{N\alpha}\right)^{\xi} - 1 = \frac{\xi(x_\alpha - u)}{\sigma} \qquad (8)$$

Finally – given an empirically observed exceedence count n above a chosen threshold u, plus a selected value for ξ and standard deviation σ computed as usual from the sample population of size N – the maximum error that could occur with probability α – our VaR – is estimated as

$$x_\alpha = u + \frac{\sigma}{\xi}\left\{\left(\frac{n}{N\alpha}\right)^{\xi} - 1\right\}, x_\alpha > u \qquad (9)$$

in conformance (with considerable differences of convention taken into account) to Eq (1.8) of [4].

Differences in convention just mentioned, plus the notational inconsistencies also noted previously, combine with additional subtleties and nuances within the references cited. Collectively these necessitate very close attention to meaning and intent while extracting the requisite information. First, the cited references use α in the usual context involving statistical confidence (discussed next) *and also* to represent the tail index. The latter representation is *not* employed here; symbol α herein has only one meaning. The next key issue is the standard distinction between probability and confidence;

· probability applies to outcomes from infinite sample sets.
· confidence, a compounded concept, involves statistical inferences drawn from finite sample counts.

A classical statistical connection exists between confidence level and notation $1 - \alpha$, but extreme value distribution functions are estimated, not actually known. Thus $1 - \alpha$ is appropriately associated here with quantiles rather than rigorously evaluated confidence values. To illustrate:

· MATLAB function pgev.m in Section 2.1.7 of [4] uses Eq. (1) to evaluate $H(x - u)$ at 95% cumulative probability.
· MATLAB function pgpd.m in Section 2.1.8 of [4] uses Eq. (2) to evaluate $G(x - u)$ at 95% cumulative probability.

Also in regard to notation: for further connection among these different references with their different nomenclature, Eq. (1.8) in [4] uses $q > F(x)$ for probability corresponding to a tail percentile at x_α. Two of the same authors then use $q = (1 - \alpha)$ in Eq. (11) on page 11 of [5]; $VaR(\alpha)$ is expressed as the sum of the mean plus $\sigma F^{-1}(\alpha)$, where the inverse of F with argument $(\alpha$ – typically 1% or 5%) is the $(q = 1 - \alpha)^{th}$ quantile {although that relation appears in a variance-covariance (rather than extreme value) formulation, its development is for VaR}. The resulting

expressions from [4] and [5] (again, with close attention to notational inconsistencies – including even upper and lower case usage for n and N) correspond to Eq. (9) here.

Material presented here thus far, then, involves probabilities and, for finite sample sets, quantiles rather than confidence levels. Confidence intervals are applied to estimated values for σ and ξ, through developments appearing in [7] and noted in [4]. As long as $\xi > -0.5$ the standard errors for those estimates can be obtained via maximum-likelihood methods. Note that this does not tie maximum-likelihood to the Extreme Value distribution function, but only to its parameter estimates – which in [7] are
· shown to be asymptotically normally distributed
· used in further derivations applying corresponding confidence intervals to the quantiles themselves.

That extended development enables MATLAB function `gpd_q.m` in Section 2.3.1 of [4] to calculate confidence intervals for GPD quantiles. An example is then given showing 95% confidence bounds for 0.999 tail probability. Another issue not always made clear in the literature involves distinctions among different Pareto distribution types. Further insights are fortunately provided in [4]:
· There is an ordinary Pareto distribution with $\xi > 0$ (that is the case of interest here).
· A GPD with ξ very near 0 corresponds to an exponential distribution. That is consistent with appearance of the exponential within the Gumbel distribution types.
· There is a Pareto II-type distribution with $\xi < 0$. Even those cases can be considered within the realm of "heavy-tailed" distributions if $\xi > -0.5$.
· For $\xi > 0$ the expected value of ξ^k is infinite for $k > \frac{1}{\xi}$. Thus if $\xi > +0.5$, the variance is infinite. If $\xi > +0.25$ the kurtosis is infinite. These factors will of course be taken into account in this IMU coast application.

Determination of confidence for specified tail probabilities, as just described, comes very close to just the capability needed – in a qualitative sense. Quantitatively, however, two issues need further consideration; those items and proposed steps toward solution follow:
· 0.999 is much lower than acceptable containment probability values – and sample sizes needed to establish quantiles with "many more nines" can be quite large. Rather than prescribing impractical data sets, though, it is noted that the plot in Figure 17 of [4] approaches a fairly straight line. Extrapolation offers a possible way to reach farther out on the tails.
· At any confidence level (*e.g.*, 99%) there is a small-but-not-at-all-negligible (*e.g.*, 1%) chance for being out of the interval range. *How far* beyond range is not clear from available statistical models. Addressing that issue is deferred (see **Possible Future Extensions**).

At this point, overall subject matter can be subdivided into two main categories – *i.e.*, 1) acquisition of data, and 2) analysis of the data obtained by presently known means – with a third topic (refinements or extensions) deferred to a later section. Immediate plans call for generating random sets from the IMU coast simulation defined and programmed in [8]. Those data sets will then be processed in accordance with the following design decisions:
1) Fréchet ($\xi > 0$) distributions can determine *VaR*'s far beyond the range of available data. Gumbel ($\xi = 0$) and Weibull ($\xi < 0$) distribution classes have much less importance in this investigation.
2) With no correlation *within* sample sets at 5, 10, 15, 20 ⋯ minutes, groups of results at 5-minute multiples can be analyzed separately.
3) Using different initial headings can help to mitigate introduction of correlations into the simulated IMU coast data. To maintain validity of comparisons, all flight paths will be congruent, with a procedure turn used for missed approach. The turn is to be immediately
   · preceded by GNSS cutoff
   · followed by a free-inertial straight course leg.
4) Using MATLAB functions from [4] as needed, steps listed here will yield *VaR* values – maximum error that could occur with probability α – for each coast duration.

FREE-INERTIAL ERROR SOURCES

Applying Extreme Value Theory to free-inertial coast is necessitated by the *mixed gaussian* nature [11] of the error contributors. That is, each error source is reasonably characterized as coming from a gaussian ensemble – but the ensembles have different variances. Extreme value probabilities are consequently higher than corresponding probabilities obtained from a normal distribution. For a formal assessment of this fundamental reality page 178 of [11] provides a definition and basic features. Presented here is an adaptation of that material, with notation modified to avoid conflict with other symbols used in this development:

X is a $K \times 1$ random vector and **M** is a $K \times K$ *random* matrix – a positive semidefinite "mixing parameter" in [11]; here a more restrictive positive definite condition is chosen. Its randomness provides a way to formalize variations among cumulative distribution function (cdf) parameters. Those variations produce tails that don't conform to a normal gaussian cdf. When the distribution of **X** given **M** is K-dimensional gaussian with "centre" μ and covariance matrix **M**, then the marginal distribution of **X** is mixed gaussian.

A highly important property is noted in [11] – the statistic

$$\langle s^2 \rangle = (\mathbf{X} - \mu)^{\mathrm{T}} \mathbf{M}^{-1} (\mathbf{X} - \mu) \qquad (10)$$

is distributed as χ^2 with K degrees of freedom (K - not K^2 - misprint in [11] acknowledged by its author). Reasoning is as follows: this trait clearly holds for fixed $\mathbf{M}$ and, since the conditional distribution does not depend on $\mathbf{M}$, it also holds marginally. This is a powerful generalization of a trait well known from the restrictive (fixed parameter) case.

In combination with Eqs. (II.20, 21) of [8], Eq. (10) could help to analyze $\langle s^2 \rangle$ at least in the restrictive case of zero mean for every sample run ("centre" μ identically zero). That is not pursued, however, for the following reasons:
· The analysis in APPENDIX II.B of [8] was written only as backup to the APPENDIX II.A program preceding it. That analysis is less general than the program (see closing paragraphs of APPENDIX 2.A.1 and 2.B).
· The program just mentioned is complete only after addition of effects covered in Table 4.2 of [8].
· Combining a model just described with a random matrix in Eq. (10) is nontrivial; simulation is used instead.

In this application the elements of $\mathbf{X}$ – variable(s) under investigation – come from three main categories that drive free-inertial error, *i.e.*, vertical deflections, accelerometer inaccuracies, and combined (gyro + computational) drifts. The last two subdivide further; total inertial instrument errors – even the "biases" – include several rectification effects from vibrations, both translational and rotational. What necessitates mixed gaussian modeling isn't just randomness of the vibration waveforms. Among flights in different areas at different times with different equipment, wide variations exist in the vibration spectra themselves and also in the sensitivity coefficients acting on them. Even if correlation issues (*e.g.*, from commonly traversed gravity fields) are ignored, at least the variances for instrument coefficients can be randomly selected, from some overall spec-derived ensemble, for each separate trial. The wide variety of individual contributors to overall degradation, noted in Section 4.B.2 of [8], gives ample reason to expect mixed gaussian characteristics in the results.

Although each ensemble used to sample error-generating parameters will have zero mean *over all flights*, many can produce *within each separate flight* time-varying accelerometer and gyro bias components with nonzero average *over one flight duration*. These can include effects that are motion-independent (*e.g.,* random walks with time constants not necessarily uniform) and/or motion-dependent (*e.g.,* nonzero mounting misalignments, imperfect scaling, etc.). With the random elements separately initialized (either at zero or drawn from a zero-mean ensemble) and built up as a simple Markov process, the ensemble average would automatically be maintained at zero.

VALUE-AT-RISK DETERMINATION

Steps just described will produce mixed gaussian outputs which, as noted in [4], fall within the Fréchet class of distributions. Usage as inputs to the free-inertial coast simulation will yield *VaR* values for each separate coast duration as previously noted. The *VaR* values, as shown in Eq. (9), conform to a simple relation – the sum of a threshold u plus σ amplified by a multiplying factor. Multipliers from sets of $\frac{n}{N}$ values [*0.0001, 0.0003, 0.001*], with a value for ξ of 0.3, are plotted in Figure 1.
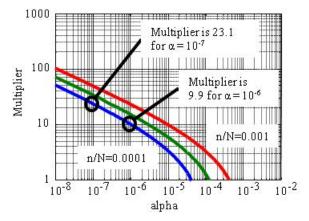

Figure 1. σ Multiplier for $\xi = 0.3$

For a shape parameter of $\xi = 0.3$, a maximum allowable α of 10^{-7} is satisfied above 23.1σ beyond threshold for $\frac{n}{N}$ at *0.0001* {in the group of curves, the top curve is for $\frac{n}{N} = 0.001$ and the lower curve is for $\frac{n}{N} = 0.0001$ }. The more above-threshold events in the observed samples, the greater the established tendency for high values to appear.

The plotted results clearly exhibit capability to extend statistical analysis beyond the range of available observations. Credibility of the resulting inferences would likely be greater for lower multiples of σ – that seems to follow from the fact, noted after Eq.(4), that an unknown distribution function can be represented only in terms of the empirically observed fraction $\frac{n}{N}$. Excessively large multiples can be avoided in practice by
· high threshold settings that disallow large $\frac{n}{N}$
· accepting values of α that are not extremely low.

The first of these steps makes a case for large sample population sizes (*e.g.*, sets of 10^5 1-hr simulation runs – roughly comparable to the number of flight-hours / day) to maintain reliability of results. The second tends to limit

how far those observations should be extended – *e.g.*, attempts to pin down a precise *VaR* for a one-chance-in-a-billion event will obviously present challenges.

Methods of obtaining all parameter values will now be summarized.   From the large Monte Carlo coast simulation run set, satisfying the desire for small values of $\frac{n}{N}$ – *0.0001* or less – the procedure is as follows:

· Extraction of nav errors after a certain coast duration, which will be taken as 30 min for two scenarios. For each scenario, complete the following steps:
· Computation of σ from the time history for the 30-min duration, via the standard relation.
· Determination of ξ for the 30-min time history, with the aid of the plot functions as illustrated in [4].
· Usage of MATLAB function findthresh.m. to obtain the threshold causing a chosen fraction $\frac{n}{N}$
· Generation of a plot of the type just shown, to provide appropriate σ-multiples for the specific ξ and $\frac{n}{N}$
· Addition of the threshold to the multiples of σ, producing the *VaR* values for α at $10^{-7}, \ldots, 10^{-5}$.

The bounding distributions will then be plotted for each of the simulation scenarios.

FREE-INERTIAL SIMULATION

As detailed in [8], initialization of the free-inertial simulation considers the following balance resulting from obtaining zero velocity error:

$$\Psi \times A + N_A = 0, \text{ for } t < 0 \qquad (10)$$

Where Ψ is the misorientation vector, A is the specific force in locally-level coordinates, and N_A is the total acceleration error. Error sources considered are:

· Gyro drift rate components modeled as first-order processes with a 1-hr time constant and selected RMS noise
· Accelerometer offset modeled as first-order processes with a 1-hr time constant and selected RMS noise
· Gyro scale factor error and uncompensated projections along the other two gyros' intended input axes
· Gravity anomalies and vertical deflections with a 20-nmi correlation distance
· Initial heading error

Table 1 summarizes the error sources and the results from 100 Monte Carlo runs, where the performance numbers are the standard deviations after 1 hr over the 100 runs. The flight trajectory consists of a 180° turn followed by straight and level flight. The aircraft speed is 200 knots, while the gyro and accelerometer scale errors are set to zero. The first five rows in Table 1 show the contributions of each of the five major error sources. Row 6 shows the combined contributions of the five error sources. Scenario

1 is represented by row 7, where the gyro drift rate is doubled to 0.02 °/hr. Scenario 2 is represented by row 8, where the gyro yaw misalignment has been increased 10-fold from 10 μrad to 100 μrad. Gyro mounting misalignment is shown to be a major concern for free-inertial coast in [12].

Table 1. Free-Inertial Simulation Parameters and Performance after 1-hr Coast

ID	Simulation Parameters	East (nmi)	North (nmi)
1	Gyro only: 0.01 deg/hr	0.38	0.32
2	Accel only: 0.03 milli-g	0.39	0.40
3	Grav anomaly only: 2 arc-sec	0.45	0.41
4	Heading error only: 0.2 mrad	0.35	0.02
5	Yaw misalign only: 0.01 mrad	0.12	0.00
6	1, 2, 3, 4, 5	0.67	0.60
7	2, 3, 4, 5, Gyro: 0.02 deg/hr	0.98	0.80
8	1, 2, 3, 4, Yaw misalign: 0.1 mrad	1.33	0.67

Next, the two scenarios were run 100,000 times where 90% of the runs used nominal errors (row 6 of Table 1), while 10% of the runs used larger errors for gyro drift and yaw misalignment, respectively. The time duration for each scenario was 30 min and the maximum nav errors were recorded that occurred during the 30-min coast duration. Figure 2 shows the East position errors for scenario 1 for all 100,000 runs, while Figure 3 shows the East position errors for scenario 2. The standard deviation for scenario 1 is 1.60 km, while the standard deviation for scenario 2 is 1.95 km.
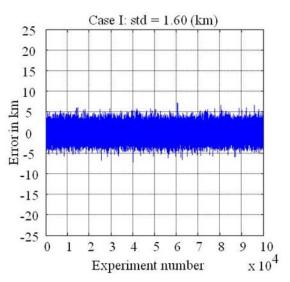

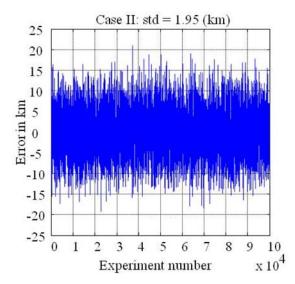Figure 2. Free-Inertial East Errors after 30 min Coast for Scenario 1

Figure 3. Free-Inertial East Errors after 30 min Coast for Scenario 2

The one-sided complement of the cdfs are plotted in figures 4 and 5 for each of the two scenarios. The solid line represents the actual data, while the dashed line represents the complement of the gaussian cdf calculated from the standard deviation of the data. Scenario 1 has the appearance of a gaussian distribution. Scenario 2 on the other hand, shows data points well in excess of that expected from a gaussian distribution.
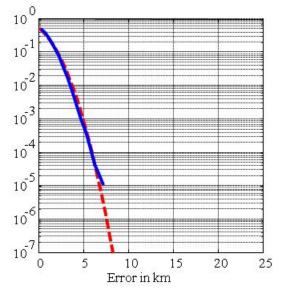

Figure 4. One-sided Complement of Free-Inertial East Error CDF after 30 min Coast for Scenario 1
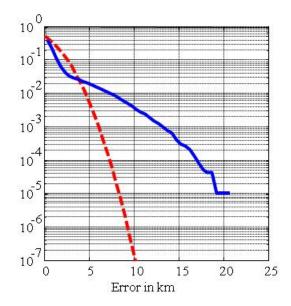

Figure 5. One-sided Complement of Free-Inertial East Error CDF after 30 min Coast for Scenario 2

For scenario 1, the shape parameter ξ was estimated to be 0.075 with a 95% upper bound of 0.11. For scenario 2, the shape parameter was estimated to be 0.06 with a 95% upper bound of 0.15. Finally, the containment bounds were calculated and are shown in figures 6 and 7 for the two scenarios.
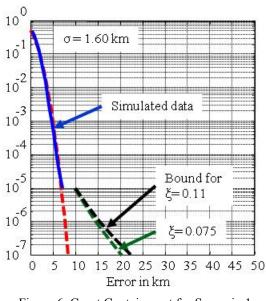

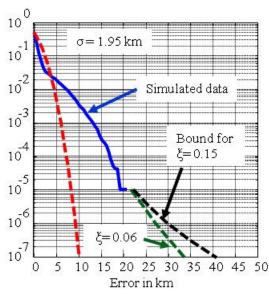Figure 6. Coast Containment for Scenario 1

Figure 7. Coast Containment for Scenario 2

Possible Future Extensions:

The good-but-not-perfect confidence levels described earlier lessen the rigor that can be attached to results produced through the methods used here. The ramifications could be studied further in the future.

As an alternative to separate sample sets at different times, theoretical means of using time-varying parameters to hold all data in one set are offered in [6]. At present there is no clear and rigorous way to define functions to represent the time-varying parameters (even the methods for estimating fixed values were until now untried for coast applications). If time-varying ξ values develop in the future, they could enable consolidation of data from unequal coast durations.

The main theory was developed for independent identically distributed ("iid") samples. The independence condition can be relaxed as in [9]. The identically distributed condition could also be relaxed – theoretically.

Multivariate EVT deals with vector-valued (rather than scalar) variables, analogous to a portfolio rather than a single stock investment. Conceivably this might be used for concurrent analysis of two features (*e.g.*, along-track and cross-track error), or multiple features. In the two-feature instance, the "track" direction would presumably be chosen in conformance to the time immediately before or after the procedure turn. Rather than using multivariate EVT forms, behavior of multiple variables (e.g., along-track or cross-track errors) can be analyzed separately.

None of these extensions are included in the present development. The immediate objective is to begin introducing EVT into free-inertial coast evaluation.

CONCLUSIONS

Extreme Value Theory (EVT) has great promise for application to free-inertial coast containment. Gyro mounting misalignment is shown to be a major concern. Practical containment bounds out to 10^{-7} exceedance probability are obtained based on experimental data from 10^5 Monte Carlo simulation runs.

ACKNOWLEDGMENTS

REFERENCES

[1] de Haan and Ferreira, *Extreme Value Theory – an Introduction*, Springer, 2006. Errata http://www.isa.utl.pt/mathemati/anath/anath.html?

[2] Ober, P.B., et al., "Statistical Validation of SBAS Integrity," European Navigation Conference, 2004.

[3] Azaïs, J.M., et al., "GNSS Integrity Achievement by using Extreme Value Theory," Proceedings of ION GNSS 2009.

[4] Gençay, Selçuk, and Ulugülyağci, "EVIM: A Software Package for Extreme Value Analysis in MATLAB," *Studies in Nonlinear Dynamics and Econometrics, 2001.*

[5] Gençay and Selçuk, "Extreme Value Theory and Value-at-Risk - Relative Performance in Emerging Markets," Int'l. Journal of Forecasting 2004, pp.287-303.

[6] Smith, R.L., "Measuring Risk with Extreme Value Theory," working paper, North Carolina University, Dept of Statistics.

[7] Hosking & Wallis, "Parameter and Quantile Estimation for the Generalized Pareto Distribution," *Technometrics* 29: 339-349.

[8] Farrell, J.L., *GNSS Aided Navigation and Tracking*, American Literary Press 2007. (http://jameslfarrell.com/published-books-gnss-aided-navigation-and-tracking).

[9] McNeil, A.J., "Estimating the tails of loss severity distributions using Extreme Value Theory," ASTIN Bulletin 27:117-137, 1997.

[10] Smith, R.L., "Extreme Value Theory," www.stat.unc.edu/faculty/rs/talks/AMS2009.pdf:

[11] Johansen, S., *Likelihood-based inference in cointegrated vector auto-regressive models*, Oxford Univ. Press, 1995.

[12] Farrell, J.L., et al., "IMU Coast: Not a Silver Bullet," Proceedings of ION Annual Meeting, 1999.